

Supplementary information

Long-term aerosol particle depolarization ratio measurements with Halo Doppler lidar

5 Viet Le¹, Hannah Lobo¹, Ewan J. O'Connor¹, Ville Vakkari^{1,2}

¹Finnish Meteorological Institute, Helsinki, 00101, Finland

²Atmospheric Chemistry Research Group, Chemical Resource Beneficiation, North-West University, Potchefstroom, 2520, South Africa

Correspondence to: Viet Le (viet.le@fmi.fi)

10 S1 Saturation at cloud base

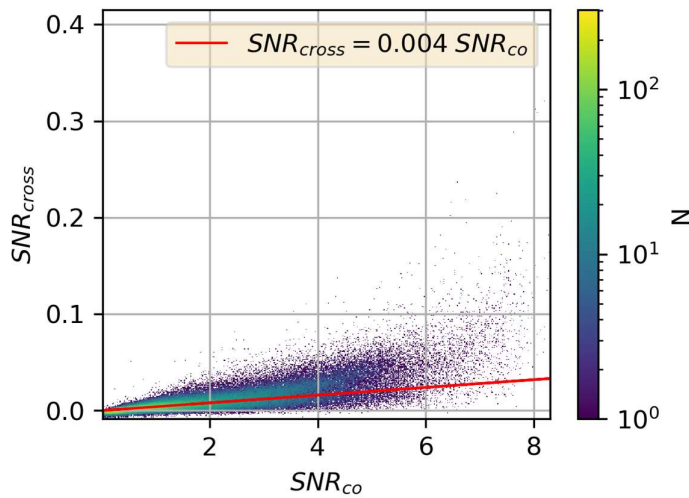
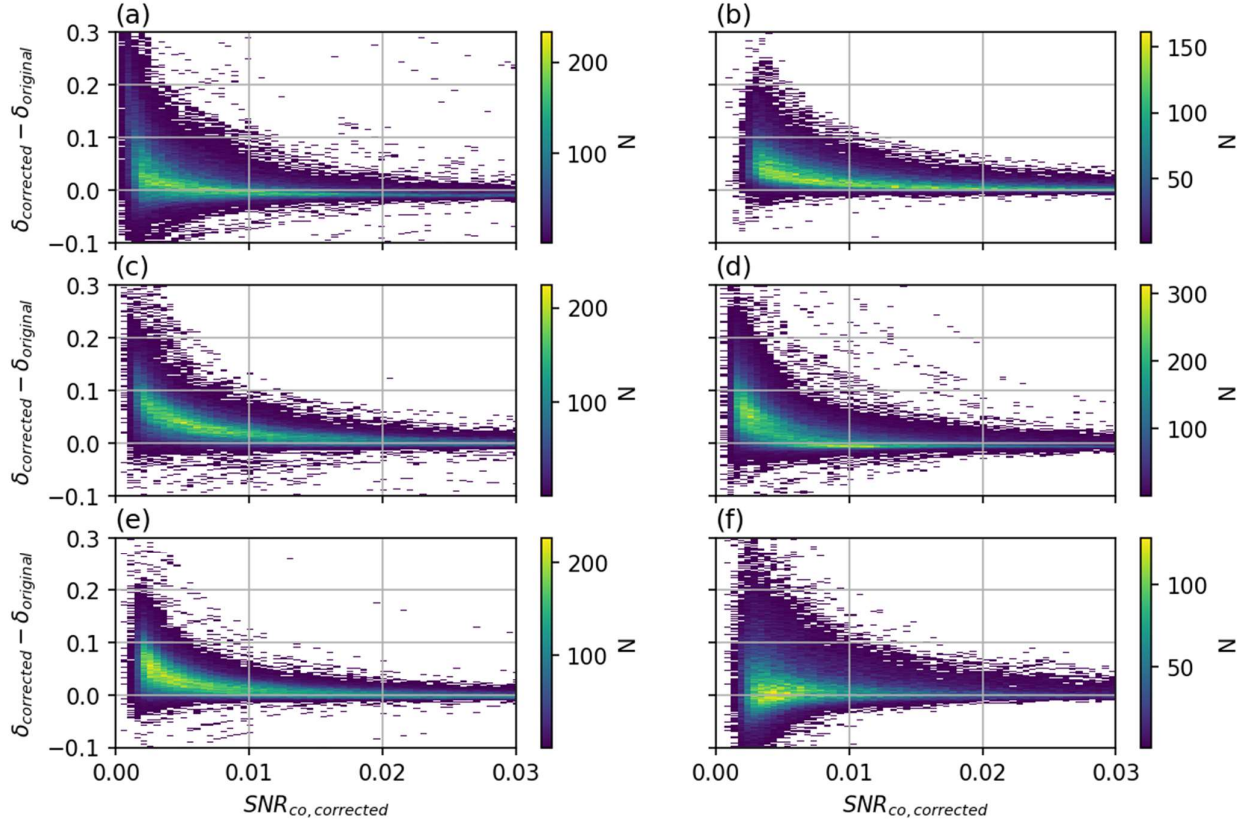


Figure S1: SNR_{co} and SNR_{cross} measured by Utö-32XR at the cloud base

S2 The effect of 2nd order polynomial component in background

15 Fig. S2 demonstrates the impact of the background correction to $\delta_{aerosol}$. For all the instruments except Sodankylä-54, the background correction increases $\delta_{aerosol}$. The increase is higher for aerosol with weaker co-SNR. The effect is negligible for strong aerosol signal with co-SNR larger than 0.01. Table S2 shows the percentage of data affected by this background correction. The effect is most prominent for instruments at Hyytiälä, with 31.8% and 24.6% of the aerosol data that have $\delta_{aerosol}$ changes by 0.05 for Hyytiälä-33 and Hyytiälä-46 respectively. However, significant changes of $\delta_{aerosol}$ by 0.1 is only at 9.3% and 7.1% of all the aerosol data for these instruments. This
20 result shows the importance of background correction in the retrieval of weak aerosol signals. Without it, biases from the 2nd order polynomial component in the background would propagate into the $\delta_{aerosol}$.



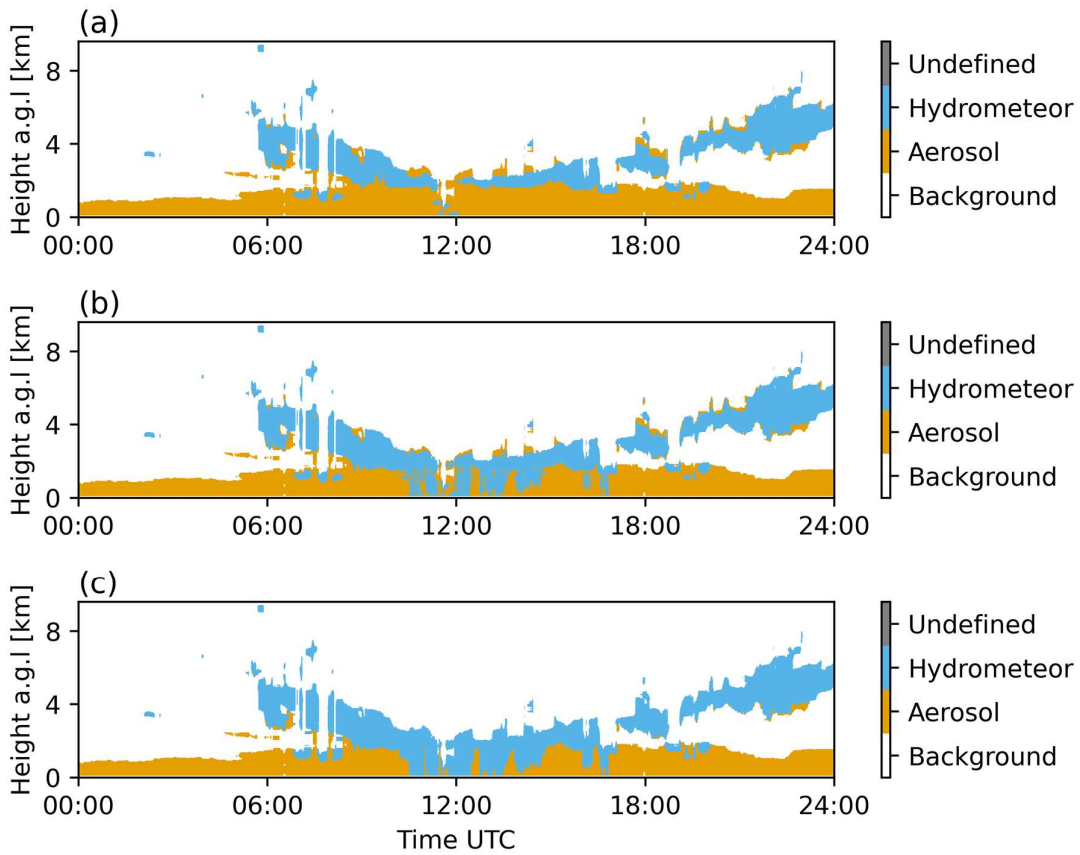
25

Figure S2: Changes in $\delta_{aerosol}$ resulted from background correction in a) Utö-32, b) Utö-32XR, c) Hyttiälä-33, d) Hyttiälä-46, e) Vehmasmäki-53, f) Sodankylä-54

Instrument	$ \delta_{corrected} - \delta_{original} > 0.05$	$ \delta_{corrected} - \delta_{original} > 0.1$
Utö-32	18.2%	6.6%
Utö-32XR	11.0%	1.9%
Hyttiälä-33	31.8%	9.3%
Hyttiälä-46	24.6%	7.1%
Vehmasmäki-53	15.5%	2.7%
Sodankylä-54	17.9%	5.1%

Table S2: The effect of background correction on number of total data point in each instrument

S3 Aerosol identification algorithm



30

Figure S3: Steps of the aerosol identification algorithm for the case presented in Fig. 4 a) Step 1: Preliminary aerosol and hydrometeor detection, b) Step 2: Falling hydrometeor detection, c) Step 3: Attenuation correction

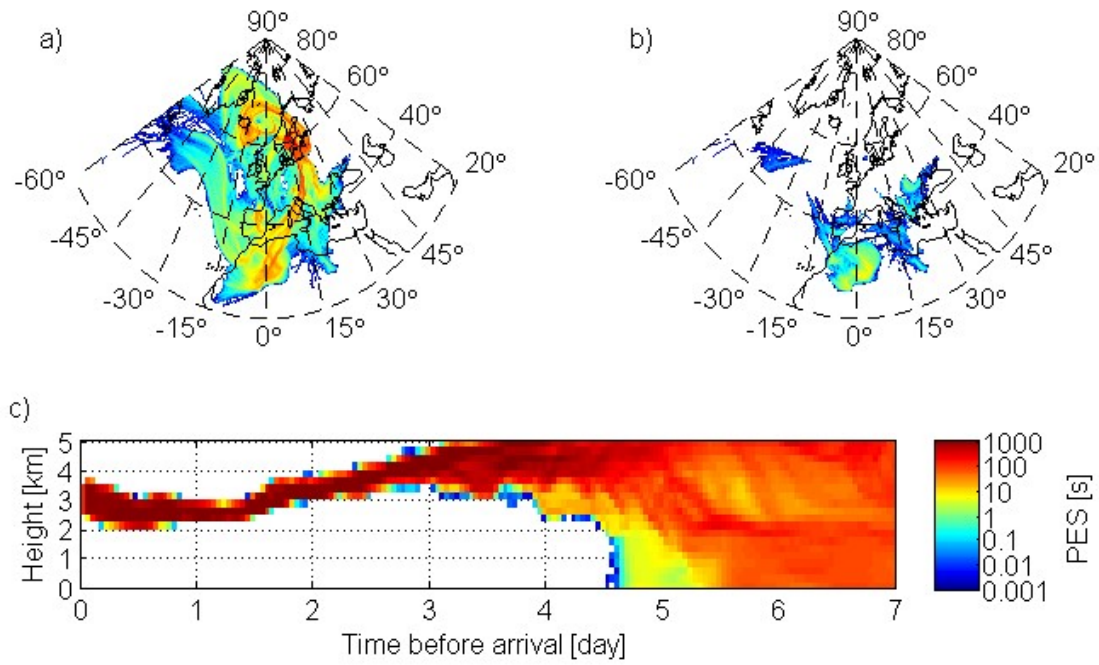
S4 The effect of relative humidity

35

Period	Location	Slope	p-value	R squared
Whole data	Utö	-0.073	$< 10^{-3}$	0.012
	Hyytiälä	-0.14	$< 10^{-3}$	0.105
	Vehmasmäki	-0.194	$< 10^{-3}$	0.219
	Sodankylä	-0.165	$< 10^{-3}$	0.142
May-June	Utö	-0.147	$< 10^{-3}$	0.045
	Hyytiälä	-0.208	$< 10^{-3}$	0.166
	Vehmasmäki	-0.169	$< 10^{-3}$	0.145
	Sodankylä	-0.127	$< 10^{-3}$	0.057

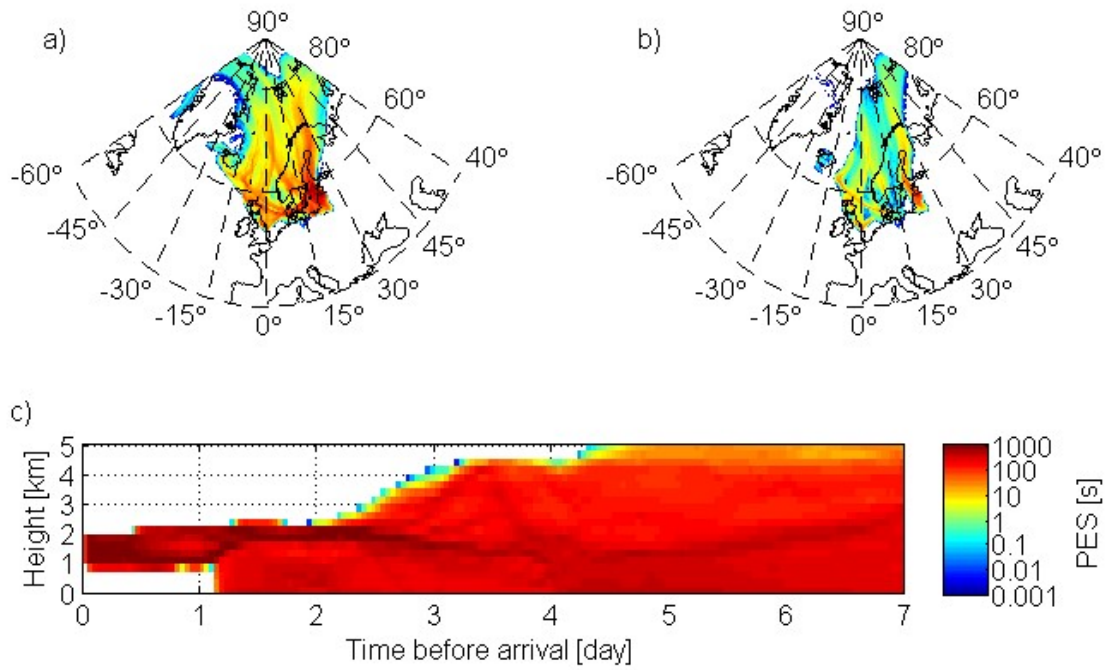
Table S4: Linear regression analysis summary for RH predicting δ_{aerosol}

S5 Hyytiälä study case



40 Figure S5: Air mass origin for the elevated layer at 2.5-3.5 km a.g.l. observed on 2018-04-15 at Hyytiälä. a) PES summed up for all heights for 7 days before arrival at Hyytiälä. b) Sum of PES in the lowest 500 m a.g.l. for 7 days before arrival at Hyytiälä. c) Vertical distribution of PES in the lowest 5 km a.g.l. for 7 days before arrival at Hyytiälä.

S6 Utö study case



45

Figure S6: Air mass origin for the elevated layer at 1-2 km a.g.l. observed on 2017-05-13 at 18 UTC at Utö. a) PES summed up for all heights for 7 days before arrival at Utö. b) Sum of PES in the lowest 500 m a.g.l. for 7 days before arrival at Utö. c) Vertical distribution of PES in the lowest 5 km a.g.l. for 7 days before arrival at Utö.